



Climate Change Projections and Impacts on Future Temperature, Precipitation, and Stream flow in the Veua Catchment, Ghana

Gemechu Fufa Arfasa^{a,b}, Ebenezer Owusu-Sekyere^b, Dzigbodi Adzo Doke^b

^a Wolaita Sodo University, Department of Natural Resource Management. P.O. Box. 138. Sodo, Ethiopia

^b Faculty of Natural Resources and Environment, Department of Environment and Sustainability Sciences, University for Development Studies, Tamale, Ghana

ARTICLE INFO

Keywords:

Climate Change
GCMs
SWAT
SSPs
Ghana

ABSTRACT

Climate change has emerged as a global challenge with varied impacts across regions. The Veua catchment, for instance, is identified as particularly susceptible to climate change due to its location and ecological fragility. This study projects climate change's impact on the area's temperature, precipitation, and stream flow. Data on temperature and precipitation obtained from the Ghana Meteorological Agency were augmented by incorporating precipitation data from twelve satellite sources using CHIRPS data with a 0.05° (5km) resolution to complement the existing in-situ datasets. The temperature data for the satellite station was sourced from the NASA power project. Modelled climate data from six GCMs, considering SSP 4.5 and SSP 8.5 emission scenarios, were retrieved from the CMIP6 data portal. R software facilitated the extraction of NetCDF-format GCM data to Excel format, and CMhyd was applied for downscaling GCM data. Temperature and precipitation bias correction utilized the variance and local intensity scaling methods, respectively. The statistical significance of changes and trends in temperature, precipitation and stream flow was determined using the Mann-Kendall (MK) method. The results indicate that temperature is expected to increase on average between 2.10 and 3.5°C under SSP4.5 and between 2.7 and 4.15°C under SSP8.5. For SSP4.5, the anticipated decrease in annual average precipitation ranges between 12.34 and 13.1%, while SSP8.5 projects a decrease of 12.6 to 13.6%. Under SSP4.5 and SSP8.5, the projected annual average stream flow will decrease by 28 to 37% and 36 to 42%, respectively. These findings suggest the need for the formulation of long-term water resource management strategies, and existing strategies should be strengthened to address the impact of climate change on the catchment.

1. Introduction

Climate change is defined as a statistically significant shift in the average climatic conditions or variability that persists for several decades or longer (Milentijević et al., 2022). Temperature changes are notable manifestations of climate change (Kwawuvi et al., 2023). Global surface temperatures have increased by 0.71°C over the past century, with significant warming in some regions (Sun et al., 2021). The IPCC has used climate simulators since its inception (Trasobares et al., 2022). According to simulations from several climate models, global temperatures may rise by 2.0 to 2.4°C above pre-industrial levels by the 21st century (Kikstra et al., 2022). At both the local and global levels, climate change is already having significant effects on streamflow, temperatures, rainfall, water availability, soil moisture, and evapotranspiration (Bokhari et al., 2018). Understanding these hydroclimatic variables is necessary to evaluate long- and short-term trends in precipitation, temperature, and streamflow data, regardless of whether the changes

are statistically significant or not, as well as to identify shifting trends due to the expected impact of climate change. Examining the current and prospective streamflow within the catchment area is of utmost importance, as well as assessing the current and future water supply. The Coupled Model Inter-comparison Project Phase 6 (CMIP6), the most recent ensemble model created by the Global Climate Models (GCMs), is currently being used. The IPCC AR6, which has been formulated following the guidelines and methods set by the IPCC, reflects the collective work of prominent specialists in the realm of climate change (Masson-Delmotte et al., 2021). Based on the scenarios offered by the Intergovernmental Panel on Climate Change (IPCC) in their Sixth Assessment Report (AR6) (Pascoe et al., 2020), these models were developed to anticipate and forecast climate change, the increase in greenhouse gas levels, and weather patterns. The models projected climate variables and changes using a set of five new climate scenarios known as shared socio-economic pathways (SSPs) (Meinshausen et al., 2020). Climate change is predicted to cause West Africa to endure

E-mail address: feragemechu@gmail.com (G.F. Arfasa).

<https://doi.org/10.1016/j.envc.2023.100813>

Received 13 October 2023; Received in revised form 8 December 2023; Accepted 9 December 2023

Available online 10 December 2023

2667-0100/© 2023 The Authors. Published by Elsevier B.V. This is an open access article under the CC BY-NC-ND license (<http://creativecommons.org/licenses/by-nc-nd/4.0/>).

constant and rising warmth (up to 6.5°C), exceeding the projected mean global temperature of 1.5°C by 2100 (Sylla et al., 2016). Ghana is one of the countries where the impacts of climate change are being seen in the rising temperatures and variable rainfall across all ecological zones (Ampadu et al., 2018). The upper east region of Ghana is hotter than the rest of the country, with an average temperature is 31.47°C (88.65°F) and it is 2.61% higher than Ghana's averages. Upper East experiences 81.37 wet days (22.29% of the time) with an average yearly precipitation of 44.5 millimeters (1.75 inches) (Boansi et al., 2023). The Veua catchment is considered to be one of the regions at high risk from the impacts of climate change. It is confronted with challenges related to sudden and extreme weather events like drought, flooding and harmattan (Larbi, Nyamekye, et al., 2020).

Veua catchment is predicted to see decreased streamflow, seasonal distribution, and rainfall owing to climate change. Surface runoff and water yield are both expected to decline by 42.7% and 38.7%, respectively (Larbi et al., 2021). Oti (2019) anticipated that between 2051 and 2080, less water will flow through the Densu River watershed as a result of climate change and variability. Several studies on the climate in the catchment were carried out, with a particular emphasis on the effects of climate change on temperature extremes and adaptation strategies, the influence on surface hydrology, and the impacts of climate change on the Veua catchment and irrigation scheme. However, there is still limited comprehensive data regarding the potential effects of future climate change on precipitation amount, seasonal distribution, and magnitude of stream flow in the Veua catchment area. The objective of this study was to evaluate and project the impacts of climate change on future rainfall and streamflow in the Veua catchment. This is based on projections of precipitation and temperature under the SSP 4.5 and SSP 8.5 climate change scenarios. In order to effectively manage water resources, ensure long-term sustainability, and build a resilient community, it is crucial to comprehend how future climate change will affect the amount of rainfall, seasonal distribution, and stream flow. This helps planners, and policymakers, along with water managers, river basin management, and environmental managers to improve their decision-making and to mitigate the future impacts of climate change in the study area.

2. Materials and methods

2.1. Description of the study area

The Veua catchment is a sub-catchment of White Volta Basin in the upper east region of Ghana and is located between latitudes 10°30'–11°08' N and longitudes 0°59'–0°45'W (Fig. 1). It has a total land area of about 305 km² and covers mainly the Bongo and Bolgatanga districts in the UER of Ghana with a small portion in the south-central part of Burkina Faso. The climate of the catchment is controlled by the movement of the Inter-Tropical Discontinuity (ITD) over the West African region (Larbi et al. (2019)). Located in a semi-arid agro-climatic zone, the catchment crosses three agro-ecological zones: The Savanna and Guinea Savanna zones in Ghana, and the north Sudanian Savanna zone in Burkina Faso (Forkuor, 2014). The catchment is characterized by an August-typical peaking uni-modal rainfall regime from May to October with a mean annual rainfall of approximately 956 mm (Larbi et al., 2018). The average annual temperature is quite hot at 28.9 degrees Celsius, and throughout most of the year, the amount of water lost through evaporation and plant transpiration is greater than the monthly rainfall. However, this is not the case during the three wettest months, which are July, August, and September (Fig. 2) (Limantol et al., 2016). The catchment has an elevation range of 89 m to 317 m (Fig. 1) whereas the LULC is mainly dominated by cropland followed by grassland interspersed with shrubs and trees. Agriculture, is the main activity of the people in the catchment (Larbi et al., 2019).

2.2. Data used for this study

2.2.1. Geospatial data

Digital elevation model data for the catchment has been uploaded with a resolution of 30 m x 30 m at <https://glovis.usgs.gov/app> (Fig. 3). A digital map of LULC was used to observe the heterogeneity of the catchment. The model needs LULC types to create land-use databases, produce land-use attributes, and simulate streamflow. A soil map was obtained from FAO soil data base. A soil map was utilized to create soil

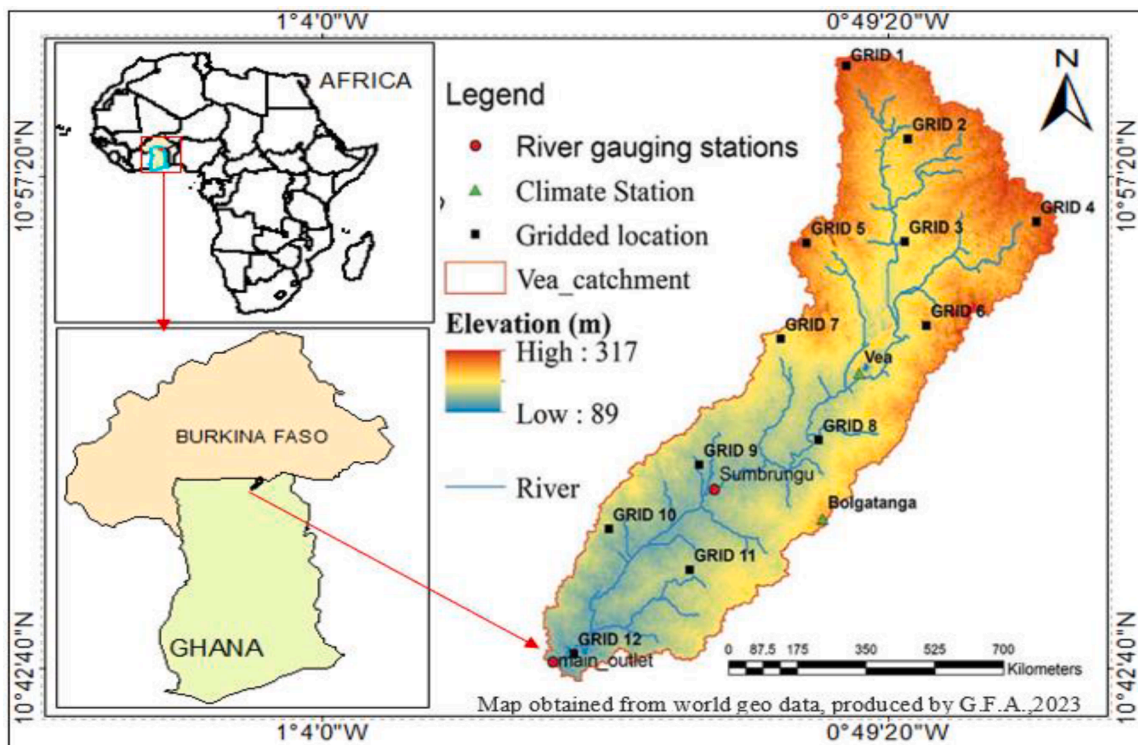


Fig. 1. Map of the study area with the distribution of meteorological stations.

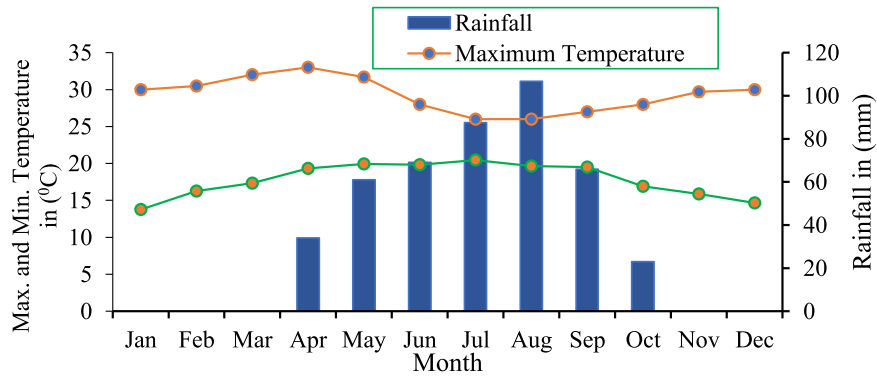


Fig. 2. Monthly average temperature and precipitation of Veia catchment.

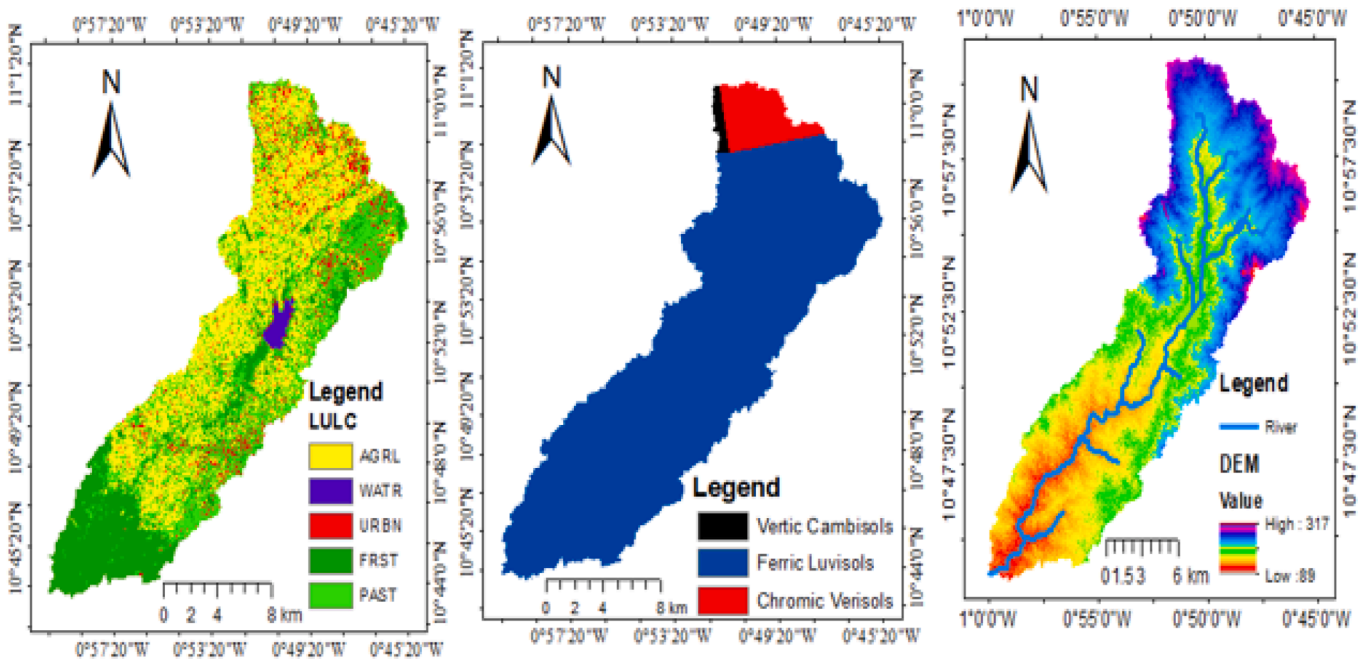


Fig. 3. LULC map, Soil map and DEM of the study area.

databases, categorize different types of soil, determine the chemical and physical properties of the soil, and stimulate the streamflow. A digital soil map was used to account for the heterogeneity of the catchment. The basin was delineated automatically in ArcGIS 10.7 using an acquired DEM with the projection type set as Transverse Mercator and spheroid type set as WGM 84. The characteristics of the hydro - meteorological and other data used in setting up and running the SWAT simulations are summarized in (Table 1).

2.2.2. Climate data (observation and scenarios)

Historical daily rainfall, maximum and minimum temperature covering the period from 1993 to 2022 for the Veia, and Bolgatanga automatic weather stations within the Veia catchment and a river water level gauge (Sumburugu) were obtained from the Ghana Meteorological Agency. Climate data is required to simulate streamflow for the period of

reference in the SWAT hydrological model and to evaluate the impact of climate change in the future. Due to the sparse distribution of in situ climate stations throughout the catchment, additional daily values of rainfall for 12 gridded sites were extracted from the Climate Hazards Group Infrared Precipitation with Station (CHIRPS) data to complement the in-situ datasets. CHIRPS combine satellite imagery with on-site station data to create gridded time series of rainfall at a resolution of 0.05°. The three agro ecological zones in the study area the north Sudanese Savanna zone (Grid1 and Grid2), Savanna zone (Grid3, Grid4, Grid5, Grid6, Grid7, and Grid 8), and Guinea Savanna zone (Grid9, Grid10, Grid11, and Grid12), were chosen to correspond to these gridded locations (Fig. 1). This dataset provided a good representation of real meteorological events and climate trends. The feasibility of the CHIRPS data in reproducing the climatology of the Veia catchment has been examined in a previous study by Larbi et al. (2021).

Table 1
Input data to set up and run the SWAT simulations.

No	Data type	Description	Source
1	DEM	The digital elevation model (DEM) used was the 30*30m resolution Shuttle Radar Topography Mission (SRTM)	USGS https://glovis.usgs.gov/app
2	Soil Map	Soil type and distribution for the Veua catchment was obtained at 10 km resolution	Modified FAO digital map of the world, Soil Research Institute (Ghana)
3	LULC map	Land use type and distribution for the Veua catchment with 30*30 m resolution was used	USGS https://glovis.usgs.gov/app
4	Climate data for baseline period	Daily minimum and maximum temperature (°C) Daily rainfall (mm)	GMET (Ghana), NASA https://power.larc.nasa.gov/data-access-viewer/ CHRIPS https://data.chc.ucsb.edu/products/CHIRPS-2.0/
5	Model data for future climate	Minimum and maximum daily Temperature (°C) and rainfall (mm) for CMIP6, SSPs scenarios	https://pcmdi.llnl.gov/mips/cmip6/dataportal.html/
6	Streamflow data	Daily Streamflow data (Sumburugu) used to calibrate and validate streamflow from the Veua catchment	WASCAL Bolgatanga branch office

The temperature data from the NASA POWER project are extracted from Modern Era Retrospective-Analysis for Research and Applications (MERRA-2) assimilation model products and GEOS 5.12.4 near-real-time products (Arshad et al., 2021). These two satellite products have been selected based on their ability to accurately reproduce the climatology in the Veua catchment within Ghana (Larbi et al., 2021). Data quality control in terms of missing data checks for the two climate stations was performed. Less than 10% missing data records for rainfall and temperature were found for each of the two climate stations.

2.3. Global climate models (GCMs) and climate data projections

The group of scientists studying climate change has developed a new collection of scenarios known as the SSPs. These scenarios help analyze the combined effects of future climate impacts, vulnerabilities, adaptation, and mitigation (Riahi et al., 2017). The IPCC Sixth Assessment Report (AR6) suggested five (5) approaches for analyzing and projecting various emission scenarios related to climate change. The five (5) anticipated emission scenarios are represented by a fresh set of socio-economic hypotheticals called Shared Socioeconomic Pathways (SSPs), which are SSP 1-1.9 (extremely low), SSP 1-2.6 (low), SSP 2-4.5 (moderate), SSP 3-7 (high), and SSP 5-8.5 (very high) (Collins et al., 2017; Lurton et al., 2018). In this study, Six GCM models from the Coupled

Table 2
Models to download CMIP6 climate data.

No	CMIP6 model name	Country	Horizontal resolution (long. by lat. in degrees)	Variant label
1	CanESM5	Canada	2.8° × 2.8°	r1i1p1f1
2	MPI-ESM1-2-LR	Germany	1.9° × 1.9°	r1i1p1f1
3	IPSL-CM6A	France	2.5° × 1.3°	r1i1p1f1
4	MIROC6	Japan	1.4° × 1.4°	r1i1p1f1
5	CNRM-CM6	Germany	0.9° × 0.9°	r1i1p1f1
6	NorESM2-LM	Norway	2.5° × 1.9°	r1i1p1f1

Sources: <https://pcmdi.llnl.gov/mips/cmip6/dataportal.html> (Gyamfi et al., 2021).

Model Inter-comparison project phase six (CMIP6) were used for future climate change projections and assessments under two SSP 4.5 and SSP 8.5 emission scenarios for the Veua catchment. SSP 4.5 assumes a world with increasing urbanization, improved education and economic development leading to decline in population growth rates. It is moderate carbon emission scenario. SSP 8.5 represents the future world where there is high population growth, rapid economic expansion and heavy reliance on fossil fuels. It is high carbon emission and climate signal is strongest. So for the future climate change projection, we selected SSP 4.5 and SSP 8.5. Table 2 shows GCMs models: CanESM5, CNRM-CM6-1, IPSL-CM6A-ATM-HR, MIROC6, MPI-ESM1-2-LR and NorESM2-LM were selected based on previous studies conducted in the Volta basin and Tono basin (Larbi et al., 2022; Okafor et al., 2017).

2.4. Downscaling GCM data using CMhyd and R programming

Climate projections for the future are typically generated through the use of global climate models (GCMs) (Hewitt et al., 2021). GCMs are scientific tools that replicate the complete climate system of the Earth, encompassing the oceans, atmosphere, and land. They are designed to depict large-scale climate patterns across continents and have been proven to accurately represent general patterns as observed in meteorological datasets from the 20th century (Manski et al., 2021). These GCMs offer well-configured environments for examining the impact of various future greenhouse gas emissions on the climate of the Earth. The downscaled model output is more realistic than the GCM model output for direct application as hydrological model input and regional-scale assessments for climate change impact (Orkodjo et al., 2022). R software Version 4.6.2. was used for extracting GCM data from NETCDF format to ASCII format. Downscaling from GCMs to RCMs is necessary before using GCM model data as input for the hydrological model (Dessu & Melesse, 2013). CMhyd was used for downscaling GCM to the local study area. CMhyd is a Python-based tool to enable the use of global and regional climate model data in hydrological models. It applies temporal and spatial bias correction of climate model data, so it can best represent the observation gauges used as inputs for hydrological models. CMhyd has the ability to handle fragmented time series; it is recommended to use complete time series. CMhyd has the ability to extract and correct precipitation (PCP) and temperature (TMP) data. It has the ability to automatically select the variables and the latest software that is widely used. CMhyd supports two data formats for simulated climate data (netCDF and ASCII).

2.5. Bias correction

Prior to using climatic data for models of climate change and studies on its impacts, biases typically need to be corrected (Hosseinzahtalei et al., 2021). Because, GCM model output data usually has a significant bias, which necessitates correlation to analyze data bias reduction, improve data quality, and increase data reliability (Her et al., 2019). Hydrological modeling software (CMhyd) climate model data were utilized in this study to correct bias and remove bias from future climate daily temperature and precipitation data. For this study, we downloaded CMhyd software from <https://swat.tamu.edu/software/>. The variance scaling bias-correction method was used to correct both the mean and variance of the temperature time series (Fang et al., 2015). The local intensity scaling (LOCI) method of precipitation bias correction in addition to wet-day frequencies and intensities (Smitha et al., 2018). The bias-corrected rainfall and temperature-simulated data (GCM) were used to assess the projected changes in rainfall and temperature at the Veua catchment under the SSP4.5 and SSP8.5 scenarios. The change analysis was conducted for the period 2023–2052 (Near -future), and 2071–2100 (Far- future) relative to the 1993–2022 reference period.

3. Man-Kendall (Non-Parametric) Trend Tests

The Mann-Kendall (MK) trend test is a non-parametric test used to identify trends in a series, even when there is a seasonal component in the series (Gumus et al., 2022). It is appropriate for hydrometeorological observations where data points are not homogeneous. It is used to find trends that are monotonically increasing or decreasing in the study area and determine if the trend is statistically significant or not (Gurara et al., 2022). In this study, the researchers used the two-sided homogeneity test of the R software to analyze how the patterns of precipitation, temperature, and streamflow changed over time. Also, to determine the significance levels of the data statistics and the null hypothesis for different time periods: a reference period (1993–2022), the near future (2023–2052), and far future (2071–2100). The null hypothesis (H0) suggests that the data does not show any consistent trend, while the alternative hypothesis (HA) suggests that there is a consistent trend in the data over time. To determine whether or not to accept the null hypothesis, the test's statistics were compared to the distribution. The null hypothesis rejected when Z's absolute value greater than the critical value, which indicates a certain type of error, keeping Type I error less than 5% or 10% can use tables (standard normal distribution) at a particular significance level (0.05 or 0.1). The critical value of Z 1/2 as determined by the standard normal table is 1.96 with a p-value of 0.05 or 0.1. We evaluated the significance of the observed and predicted trends in precipitation, temperature, and streamflow using various statistical measures. These measures included the Z score (measuring the number of standard deviations), the p-value (indicating the probability), and the confidence levels of -1.96 and +1.96 (representing a 95 percent level of confidence), and 0.05 (equivalent to a 95 percent level of confidence). If the P-value is less than or equal to 0.05, then the null hypothesis is considered valid. The level of statistical significance for the observed and projected precipitation, temperature, and simulated and predicted streamflow was set at 0.05.

The mathematical equations used for the standardized calculation of Z-test statistics and time, as well as statistics from the MK (Var [S]) series, calculate the variance for the corrected links (assuming P-value links in the data) using (Eq. 1) as follows:

$$S = \sum_{k=1}^{n-1} \sum_{j=k+1}^n \text{sgn}(X_j - X_k) \quad (1)$$

S = any integer between $-n(\frac{n-1}{2})$ and $n(\frac{n-1}{2})$, X_j and X_k are sequential time series values, n is the number of data in the set, $\text{sgn}(X_j - X_k)$ is the sign function and is given as:

$$\text{sgn}(X_j - X_k) = \begin{cases} 1 & \text{if } (X_j - X_k) > 0 \\ 0 & \text{if } (X_j - X_k) = 0 \\ -1 & \text{if } (X_j - X_k) < 0 \end{cases} \quad (2)$$

It is also assumed that for $n=8$, the S test statistics is normally distributed, with mean value zero and variance calculated using equation (3.17)

$$\sigma^2 = \frac{n(n-1)(2n+5)}{18} \quad (3)$$

Under this situation the standardized test statistics Z will be:

$$Z = \begin{cases} \frac{S-1}{\sigma} & \text{if } S > 0 \\ 0 & \text{if } S = 0 \\ \frac{S+1}{\sigma} & \text{if } S < 0 \end{cases} \quad (4)$$

The decision to either reject or accept the null hypothesis is then made by comparing calculated Z with the critical value at a chosen level of significance. Sen's slope estimator is also a nonparametric test by which the true slope (change per year) of a trend is estimated.

Sen's test is used when the trend is assumed to be linear, i.e.

$$f(t) = Qt + B \quad (5)$$

where $f(t)$ = increasing or decreasing function of time, i.e., the trend Qt = the slope B = intercept (constant) the slope of each data pair Q_i is calculated as:

$$Q_i = \frac{X_j - X_k}{j - k} \quad (6)$$

where, $j > k$ and, if there is n number of X_j in the time series, one can get as many as $N = \frac{n(n-1)}{2}$ slope estimates Q_i

Then the values of Q_i are ranked from small to large; the median of which is the Sen's slope (Q)

$$Q = \begin{cases} Q_{\left[\frac{(N+1)}{2}\right]} & \text{if } N \text{ is Odd} \\ \frac{1}{2} \left(Q_{\left[\frac{N}{2}\right]} + Q_{\left[\frac{(N+1)}{2}\right]} \right) & \text{if } N \text{ is even} \end{cases} \quad (7)$$

Then the values of Q_i are ranked from small to large; the median of which is Sen's slope (Q)

The 'trend' and 'Kendall' software packages of the R Libraries were used to evaluate the statistical significance of change and to detect variations in temperature, precipitation, and streamflow. This method of pattern detection and analysis is used to determine whether hydro-meteorological time series data is increasing, decreasing, or remaining constant over time (Oguntunde et al., 2017). MK test has a variety of advantages, such as being less sensitive to outliers, supporting time-series data, and requiring no input data to depict a particular distribution (Adarsh & Janga Reddy, 2015; Ebrahimian et al., 2018). It is a simple and widely used nonparametric technique for detecting monotonic upward and downward trends, as well as for analyzing the time trend of series data true values (Wang et al., 2020). Mann-Kendall trend test is a technique for determining observed, simulated, and predicted trends in precipitation, temperature, and streamflow by determining whether a trend in the data changes over a time series of meteorological and hydrological variables.

4. The Hydrological model (Soil and Water Assessment Tool (SWAT))

SWAT was developed to 'scale up' previous field-scale models to large river basins after more than 30 years of model development within

the US Department of Agriculture's Agricultural Research Service (Arnold & Fohrer, 2005; Gassman et al., 2022). The SWAT model divides a river basin into multiple sub-basins, and each sub-basin is further divided into smaller hydrological response units (HRUs) that share similar characteristics in terms of land use, slope, soil, and hydrology (Leta et al., 2021; Welde & Gebremariam, 2017; Worqlul et al., 2018). The HRU, the smallest landscaping element in SWAT, may simulate hydrological cycles and processes in each HRU. The methods employed in the model simulate surface runoff, potential evapotranspiration, hydrology, and the routing phase of the hydrological cycle (Nasiri et al., 2020). Interested in SWAT model application, model development, input data, simulation, and estimating methodologies at <http://swatmodel.tamu.edu> (Malik et al., 2022). It uses a universal water balance equation to model daily hydrological cycles and events at each HRU (Eq. 8).

$$SW_t = SW_0 + \sum_{i=1}^t (R_{day} - Q_{surf} - E_a - W_{seep} - Q_{gw}) \quad (8)$$

where SW_t is the final soil water content (mm); SW_0 is the initial soil water content on day i (mm); t is time (days); R_{day} is the amount of precipitation on day i (mm); Q_{surf} is the amount of surface runoff on day i (mm); E_a is the amount of evapotranspiration on day i (mm); W_{seep} is the amount of water entering the vadose zone from the soil profile on day i (mm); Q_{gw} is the amount of return flow on day i (mm) (Neitsch et al., 2011).

In this research, we used the ArcGIS interface Arc SWAT hydrologic model (2012 version) to assess and predict the impact of climate change on streamflow for both current and future time periods. The SWAT hydrological model was used for this study because it is a widely used tool for river basin management, streamflow assessment, and hydrological modeling (Anand et al., 2018; Anteneh et al., 2023; Desai et al., 2021; Fukunaga et al., 2015; Wang et al., 2023). The effectiveness of the SWAT model in predicting water availability and streamflow has been extensively evaluated in various regions worldwide (Rahman et al., 2022). Results have consistently demonstrated that the model is a valuable tool for assessing the impact of climate change on streamflow, both on a regional and global scale (Chen et al., 2023; Gaur et al., 2021).

The SWAT model was set up for the Vea catchment by delineating the catchment into 25 sub-catchments with an estimated total surface area of about 305.87 km², and 71 HRUs, using a 30 m digital elevation model, 10 km soil map, and 30 m classified 2022 land-use/land-cover map (Larbi, Obuobie, et al., 2020). The model was run using the observed daily climate (station and CHIRPS gridded) data for the period of 1993–2022 using the first 3 years (1993–1996) as a model warm-up period. By utilizing the equation developed by the Soil Conservation Service (SCS), an estimation of surface runoff was made. This estimation is dependent on factors such as the type of land use, the permeability of the soil, and the moisture level in the soil prior to the event (Neitsch, 2005). The ET estimation was conducted using the Hargreaves approach, which only requires the minimum and maximum temperatures as input data. Larbi et al. (2020) provide an in-depth description of the model setup, sensitivity analysis, calibration, and validation.

4.1. SWAT model uncertainty analysis, calibration, and validation

In order to properly use the SWAT model for assessing the impact of climate change, it is important to perform uncertainty analysis, model calibration, and validation. This is because the input parameters of the model are based on processes and it is important to maintain them within a realistic range of uncertainty (Brouziyne et al., 2017; Chaemiso et al., 2016). The SUFI2 program is connected to the SWAT model, which is thought to enter rainfall data, land use, soil type, parameters, and observed data (Ali et al., 2023; Le et al., 2023). Simulation uncertainty is measured using the p-factor, often known as the 95 percent prediction uncertainty (95PPU). The 95PPU is calculated using the

likelihood function of an outcome obtained using the Latin hypercube, with an average of 2.5 percent and 97.5 percent (Farokhnia et al., 2018). The r-factor, which is calculated by dividing the average thickness of the 95PPU band by the standard error of the observed data, is another method for gauging the robustness of a calibration or uncertainty analysis. The suggested P-factor and R-factor are, 0.70 and 1.50 respectively (Beygi, 2015; Shadkam et al., 2016).

The SWAT model Calibration and Uncertainty Programme (SWAT-CUP) was developed to offer tools for automatic uncertainty analysis as well as calibration and validation of the SWAT model (Carlos Mendoza et al., 2021). Generalized Likelihood Uncertainty Estimation (GLUE), Mark Chain Monte Carlo (MCMC) uncertainty analysis methods, semi-automatic Sequential Uncertainty Fitting Ver-2 (SUFI-2), Particle Swarm Optimization (POS), and Parameter Solution (ParaSol) are linked with the SWAT model. Model calibration is the process of methodically adjusting and analyzing the most essential and sensitive model parameters until the model's outputs are as accurate as possible in capturing the behavior of the system being evaluated in a basin (Abbaspour et al., 2015; Orkodjo et al., 2022). After assessing the model's calibration, the model is validated by comparing the predictions of the model to the field of observation data that was not included in the calibration, without altering the parameter values. The SUFI-2 algorithm was used in this study for model calibration, validation, and uncertainty analysis. Because it is widely used and incorporates a variety of objective functions in its uncertainty analysis and calibration technique, the SUFI-2 approach was selected for this study. The SUFI-2 algorithm for uncertainty analysis is used by the majority of SWAT CUP systems to evaluate streamflow both now and in the future as well as susceptibility, model calibration, and uncertainty (Gu et al., 2014). The scope of uncertainty is satisfied. SWAT uncertainty quantifying and communicating the degree of confidence or error in the data, assumptions, parameters, and outputs of a model or simulation.

4.2. SWAT model performance evaluation and statistical measures of criteria

In this study, the performance of the data was evaluated using the Nash Sutcliffe coefficient (NS), coefficient of determination (R²), and percent bias (PBIAS) relative to the standard deviation of the data collected. Detailed information about the performance models of the SWAT, SWAT CUP, and SUFI2 algorithms in uncertain contexts can be found on the website <https://swat.tamu.edu/software/swatcup/>. The statistical values of NS, R², and PBIAS were computed using Eqs. 9, 10, and 11 are the matching numbers. The Nash-Sutcliffe efficiency value, which has a range of 0 to 1 (Nash and Sutcliffe, 1970), is used in calculate model performance evaluation using Eq. (9).

$$NSE = 1 - \frac{\sum_i (Q_m - Q_s)_i^2}{\sum_i (Q_m - Q_s)^2} \quad (9)$$

where, n is the total number of observations, $Q_{o,i}$ and $Q_{s,i}$ are the observed and simulated discharge at the i th observation, respectively, and Q_{mean} is the mean observed data over the simulation period. The coefficient of determination is used to calculate model performance evaluation using (Eq. 10).

Table 3
Model Performance Assessment and Statistical Measures of Criteria.

Performance	NSE	R ²	PBIAS
Very Good	0.75 < NSE ≤ 1	0.5 < NSE ≤ 0	PBIAS < ±10
Good	0.65 < NSE ≤ 0.75	0.5 < NSE ≤ 0.6	±10 ≤ PBIAS < ±15
Satisfactory	0.5 < NSE ≤ 0.65	0.6 < RSR ≤ 0.7	±15 ≤ PBIAS < ±25
Unsatisfactory	NSE ≤ 0.5	RSR > 0.7	PBIAS ≥ ±25

Source: Moriasi et al., (2015).

Table 4
Hydrological input parameters, and calibrated values for the Veia catchment.

Parameters	Definition	Lower/ upper bounds	Calibrated values
HRU_SLP	Average slope steepness (m/m)	0.0-1.0	0.014
V_CN2. mgt_AGRL	Curve number for cropland,	35-90	72.5
V_CN2. mgt_RNGE	Curve number for grassland		73.5
V_CN2.mgt_ FRST	Curve number for forest/mixed vegetation.		69.0
V_ALPHA_BF. gw	Base flow alpha factor (days)	0.0-1.0	0.02
V_ESCO.hru	Soil evaporation compensation factor	0.0-1.0	0.42
R_REVAPMN. gw	Threshold depth of water in shallow aquifer for revap to occur	0.0-1000	550
SLSUBBSN.hru	Average slope length (m)	10-150	121.9
V_GWQMN.gw	Threshold depth of water in the shallow aquifer for return flow to occur (mm)	0.0-5000	2200
R_EPCO.hru	Plant uptake compensation factor	0.0-1.0	0.02
V_GW_REVAP. gw	Groundwater “revap” coefficient.	0.02-0.2	0.02
V_GW_DELAY. gw	Groundwater delay (days)	0- 500	33
R_GW_SPYLD. gw	Specific yield of the shallow aquifer (m ³ /m ³)	0.0-0.4	0.003
SURLAG.bsn	Surface runoff lag time (days)	0.0-24	2
R_RCHRGP. gw	Deep Aquifer percolation coefficient	0.0- 1.0	0.25
RDMX_FRST	Maximum rooting depth (m) for forest/mixed vegetation	0-4	3

R: parameter value is multiplied by 1+given value; V: parameter value is replaced by the calibrated value (Larbi et al., 2021).

$$R^2 = \frac{[\sum_i(Q_m - Q_s)\sum_i(Q_m - Q_s)]^2}{\sum_i(Q_{m,i} - Q_s)^2 \sum_i(Q_{m,i} - Q_s)^2} \quad (10)$$

where Q_m = Observed variable, Q_s = Simulated variable. Ranges of R^2 are from 0.0 to 1.0. Higher value of R^2 indicates better model performance. The model performs better when PBIAS is lower in size. Zero is the optimal value, while positive (negative) values reflect over-estimation (underestimation) bias in the model (Zhang et al., 2011). A representation of equation PBIAS is shown below (Eq. 11).

$$PBIAS = \frac{\sum_{i=1}^n (Q_{obs} - Q_{sim})}{\sum_{i=1}^n Q_{obs,i}} * 100 \quad (11)$$

where $Q_{s,t}$ = Simulated variables. $Q_{m,t}$ = Observed variables, and $t = 1, 2, \dots$,

SWAT Model performance evaluation and statistical measures of criteria were carried out during the calibration and validation phases, as indicated in (Table 3).

5. Results

5.1. Hydrologic parameter evaluation, model calibration, and validation

The SWAT model was used to project and simulate the changes in streamflow on an annual, seasonal, and monthly basis, as shown in

Table 5
SWAT Model evaluation for the daily Streamflow Simulated and Observed.

Model	Indices	Year	R^2	NSE	PBIAS	P-factor	R-factor
SWAT model	Calibration	2013-2016	0.82	0.83	4.1	0.34	0.25
	Validation	2017-2018	0.83	0.84	4.3	0.27	0.15

Table 4. The SWAT model was calibrated by using 16 parameter responses that were highly sensitive to streamflow magnitude and related streamflow parameters. Streamflow magnitude change settings for each parameter were adjusted (Arnold et al., 2012) as displayed in (Table 4).

The data from the measuring station, which included the average monthly streamflow, was utilized for both the calibration and validation of the SWAT model. We used the model configuration data from 2013 to 2018, with a warm-up time of three year. Warm-up time is required for modeling. Streamflow’s four-year (2013–2016) and two-year (2017–2018) periods were used for model calibration and validation, respectively. The monthly streamflow based on the observed and simulated data at the station granted well to the performance evaluation statistics of the R², NSE, and PBIAS models over the calibration and validation periods, and the model’s output is acceptable. The recommended Value of the P-factor of 1 and R-factor of 0 indicate that the simulation exactly corresponds to the measured data. Based on the recommended value, the P and R factor values, the simulated projections for the Sumburugu station were considered acceptable and the SWAT model’s calibrated trends match those of the observed streamflow (Table 5). The model’s predictions also indicate a decrease in streamflow in the catchment. The mean monthly hydrograph of the observed streamflow compared to the simulated streamflow generally demonstrates that the calibration and validation patterns of the two hydrographs are very similar. The uncertainty is acceptable, because the P-factor and R-factor values are between 0 and 1.

5.2. Evaluation of Observed Annual and Seasonal Temperature using Trend analysis

The findings of the trend test showed statistically significant positive increasing baseline annual and seasonal maximum and minimum temperature trends. The findings revealed a noteworthy positive increase trend at two meteorological gauging stations and twelve grid stations, as presented (Fig. 4).

The analysis based on MK test (Fig. 5) displays the results of the statistical monotonicity test for the seasonal average temperature trend, which revealed that all stations had a statistically significant positive trend that was increasing.

5.3. Evaluation of Projected Annual and Seasonal Temperature and Trend Analysis

The analysis of yearly and seasonal temperature variations revealed significant temperature trends in the 60-year periods of 2023-2052 and 2071-2100. The projected minimum and maximum temperatures in the catchment area were determined using the SSP 8.5 and SSP 4.5 emission scenarios for two future time periods: the near-future (2023-2052) and the far-future (2071-2100). The analysis of trends showed that both the SSP 8.5 and SSP 4.5 scenarios predicted a notable increase in the annual average temperature. The results of the trend test analysis are shown in (Figs. 6 and 7), which show that the annual minimum and maximum temperatures in the catchment area show increasing trends for the two (2) time periods under the SSP 4.5 and SSP 8.5 emission scenarios.

The projected average results from the six GCM indicate that temperatures would increase over time in comparison to the base period under the SSP 8.5 and SSP 4.5 emission scenarios. Under emission scenarios, SSP 8.5 and SSP 4.5, the mean annual temperature in the depicted catchment (Fig. 8) increased throughout the two (2) future periods relative to the reference period.

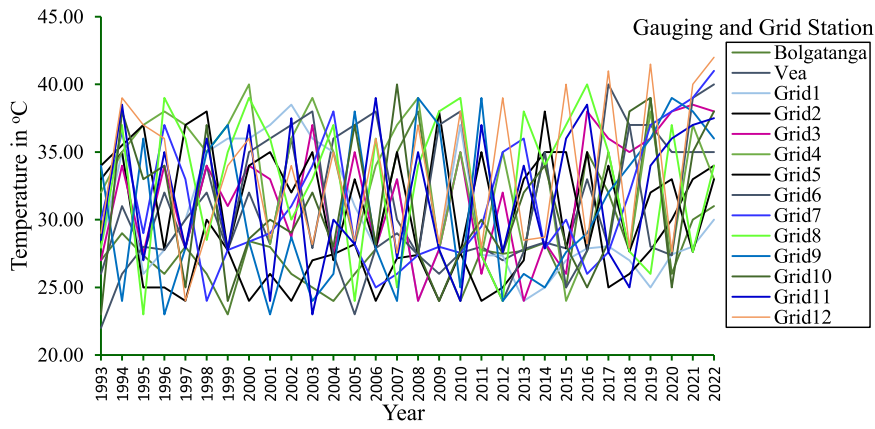


Fig. 4. Annual average temperature changes in Veia catchment during (1993-2022).

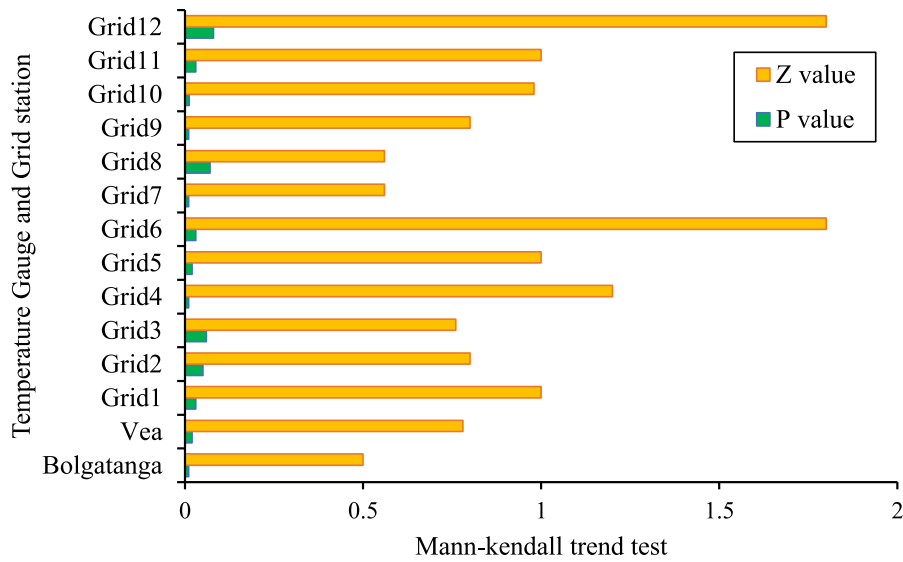


Fig. 5. Changes in average seasonal temperature in Veia catchment during (1993-2022).

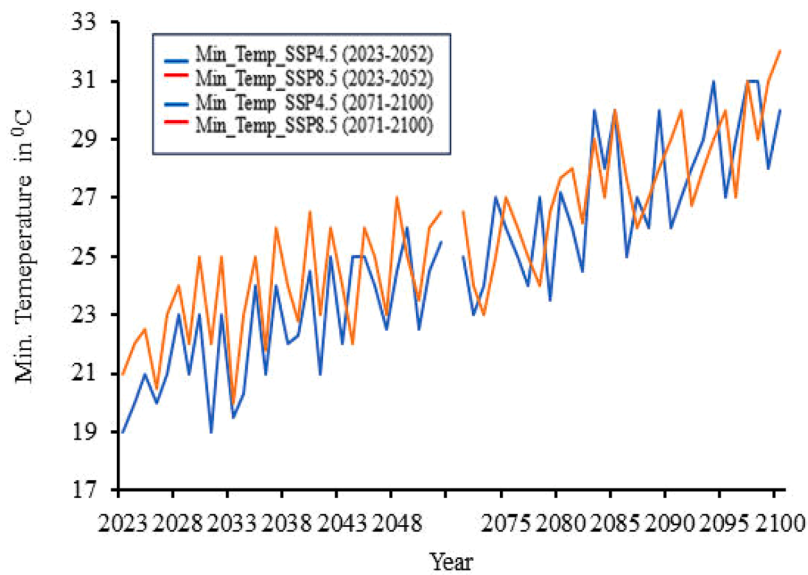


Fig. 6. Projected Change in Annual Minimum Temperature under SSP4.5 and SSP8.5 Emission Scenarios (2023-2052, and 2071-2100).

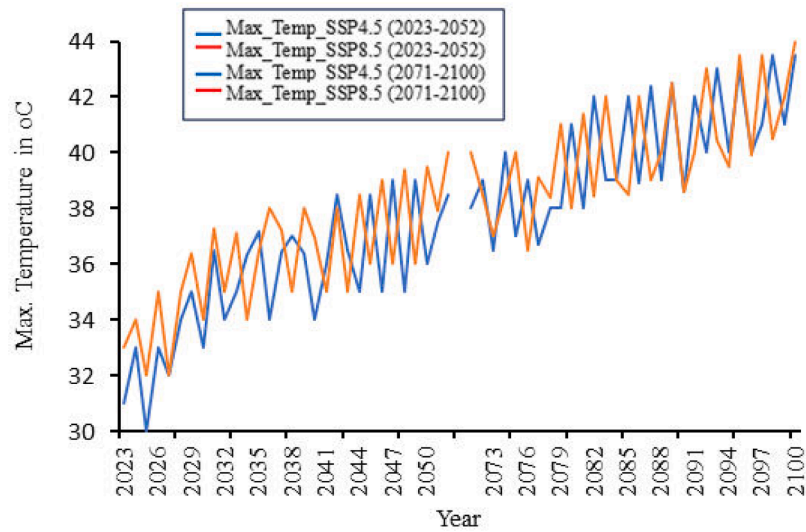


Fig. 7. Projected Change in Annual Maximum Temperature under SSP4.5 and SSP8.5 Emission Scenarios (2023-2052, and 2071-2100).

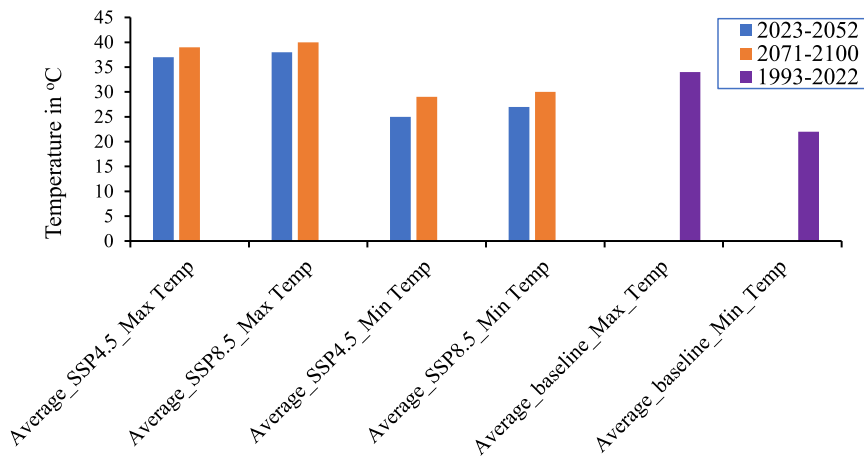


Fig. 8. Changes in Annual Average Maximum and Minimum Temperatures Projected in the SSP 4.5 and SSP 8.5 Emissions Scenarios over the Period (2023-2052 and 2071-2100) and Observed over the Period (1993-2022).

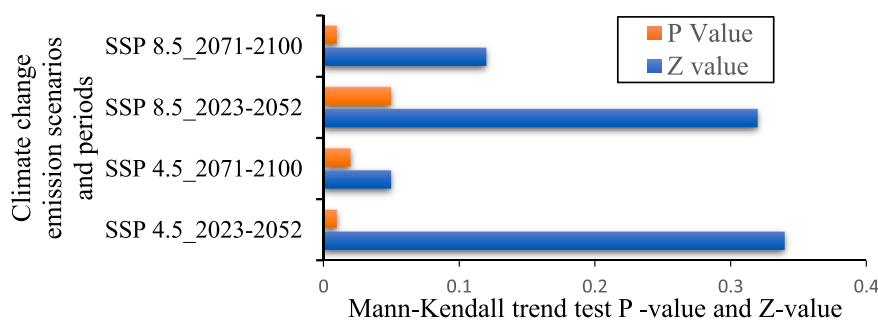


Fig. 9. Change in Projected Average Seasonal Temperature under SSP 4.5 and SSP 8.5 Emission Scenarios over the Period (2023-2052, and 2071-2100).

Based on analysis using the SSP 4.5 and SSP 8.5 emission scenarios, it is expected that the catchment will experience a significant increase in temperature under the two (2) future periods shown in (Fig. 9).

According to the SSP 8.5 and SSP 4.5 emission scenarios, it is anticipated that the monthly change in maximum (Fig. 10) and minimum (Fig. 11) temperatures will result in a significant increase over the following two (2) future periods in comparison to the base period.

5.4. Evaluation of Observed Annual and Seasonal Precipitation and Trend Analysis

Trends between 1993 and 2022 were statistically significant, according to a 30-year analysis of annual and seasonal variations in precipitation. For the baseline period, of change in precipitation trend for the Veia catchment. Two (2) precipitation measurement stations and 12

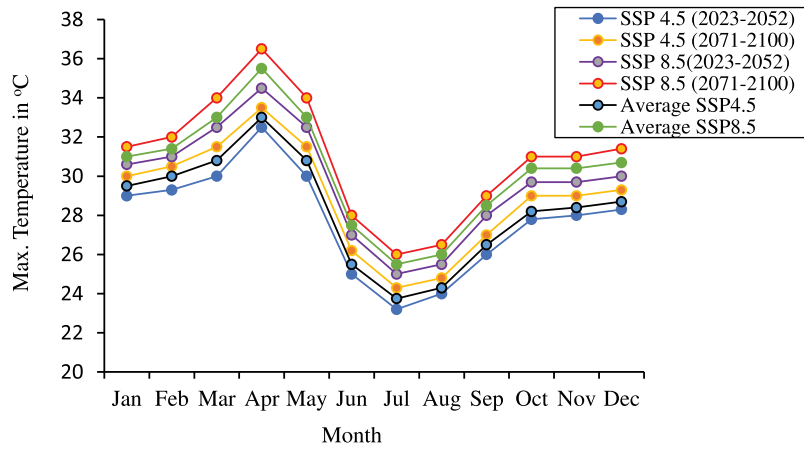


Fig. 10. Projected Changes in Monthly Maximum Temperature under SSP 4.5 and SSP 8.5 Emissions Scenarios (2023-2052, and 2071-2100).

Gridded stations from CHRIPS data were examined. For the twelve (12) grid stations and two (2) meteorological measuring stations within the basin analysis of the annual precipitation data trends of the time series showed seasonal variation trends. (Fig. 12) displayed monotonic trend changes in annual precipitation that were statistically significant, according to the trend detection test.

stations, the seasonal trend change in precipitation investigation was conducted in the Vea catchment. The nine (9) grid station and two (2) meteorological stations' data revealed a pronounced downward trend, pointing to a shift in the seasonal precipitation distribution patterns. But none of the Three (3) grid stations listed in the figure's trend detection test results (Fig. 13), found statistically significant monotonic trends in the seasonal precipitation distribution.

Using a reference period of Fourteen (14) precipitation measurement

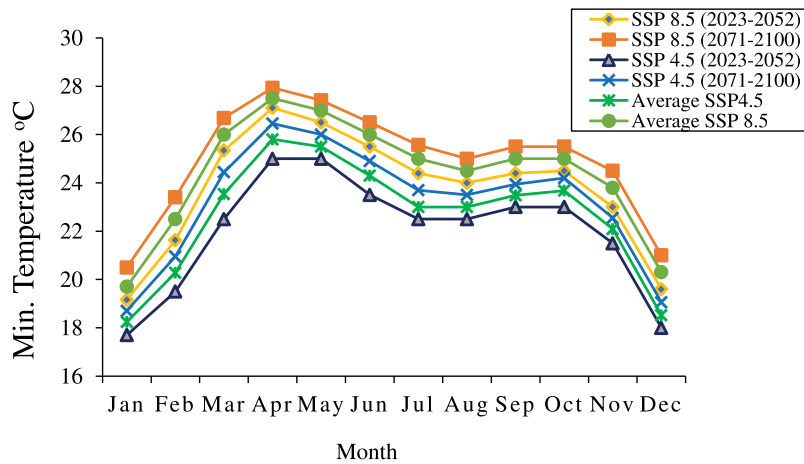


Fig. 11. Projected Changes in Monthly Minimum Temperature under SSP 4.5 and SSP 8.5 Emissions Scenarios (2023-2052, and 2071-2100).

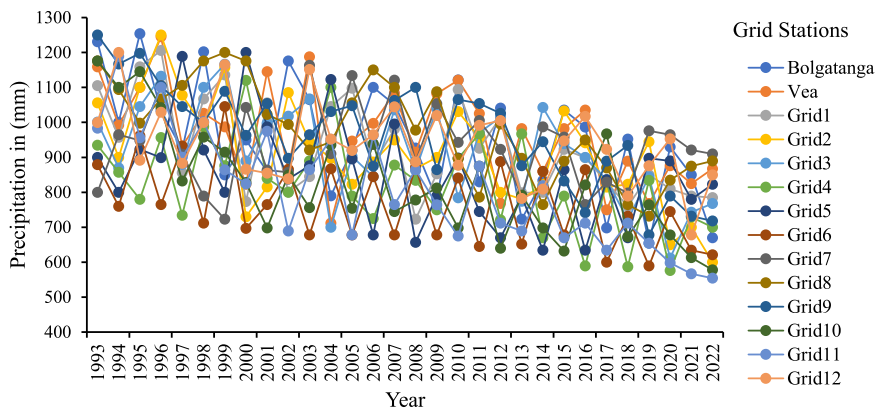


Fig. 12. Annual Precipitation in (mm) in Vea catchment during (1993–2022).

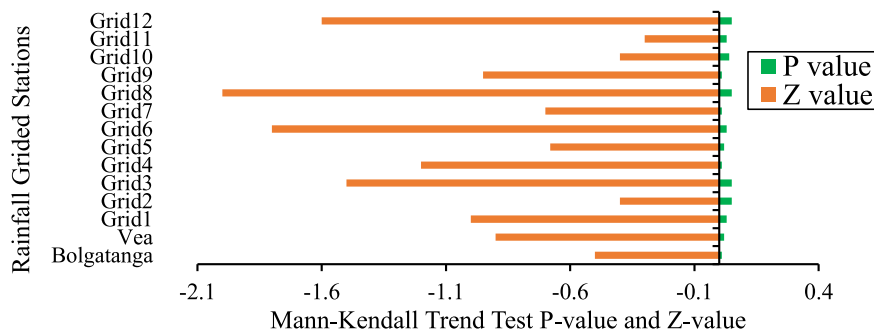


Fig. 13. Observed Seasonal Precipitation Change in Vea catchment (1993- 2022).

5.5. Evaluation of Projected Annual and Seasonal Precipitation and Trend Analysis

Statistically significant trends for the years (2023-2052 and 2071-2100) over 60 years were discovered after evaluating the change in precipitation on an annual and seasonal basis. Based on the results of the trend tests for the SSP 4.5 and SSP 8.5 emission scenarios, a significant decrease in annual precipitation amounts was predicted. The predicted precipitation for the Vea catchment was assessed for two (2) future periods: the near term (2023-2052), and the long term (2071-2100) when compared to the reference time (Fig. 14). Predicted precipitation is expected to generally trend downward in comparison to the reference period, according to the average results of the six (6) GCMs models (Table 4 and Fig. 12).

The trend test revealed that over two (2) future study periods, the

predicted seasonal precipitation distribution under the SSP 4.5 and SSP 8.5 emission scenarios showed a decreasing trend. On the other hand, this indicates that the catchment (June to August) will experience the peak rainy season as well as the erratic spring rainy season under the evaluated emission scenarios for (Fig. 15) depicts the emission scenarios for SSP8.5 and SSP4.5.

The predicted changes in monthly precipitation and monthly average precipitation over the ensuing two (2) future periods were evaluated. The average results of the six (6) GCMs models in the following two (2) periods will see a decline under the SSP 8.5 and SSP 4.5 emission scenarios (Table 4 and Fig. 16).

Under the emission scenarios SSP 8.5 and SSP 4.5, the predicted changes in precipitation in terms of annual amount and seasonal distribution were assessed and contrasted to the basin reference period for two (2) future periods (Table 6). Predicted that, compared to the

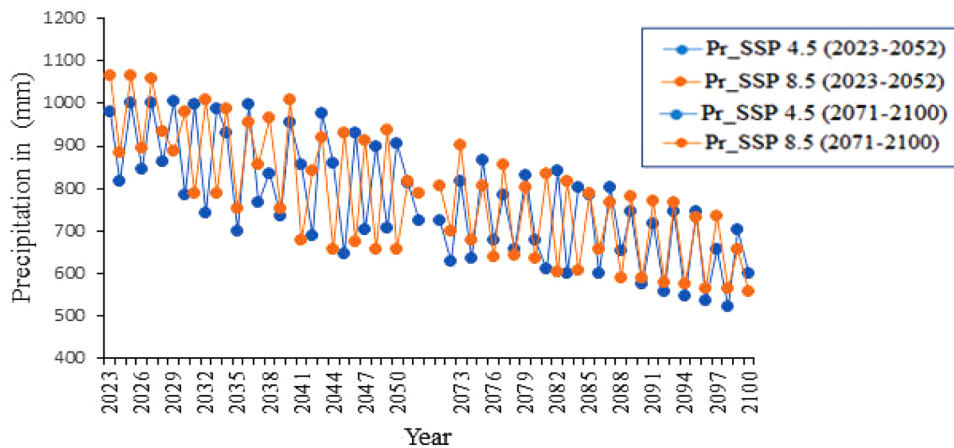


Fig. 14. Projected Changes in Annual Precipitation under SSP 4.5 and SSP 8.5 Emissions Scenarios (2023-2052, and 2071-2100).

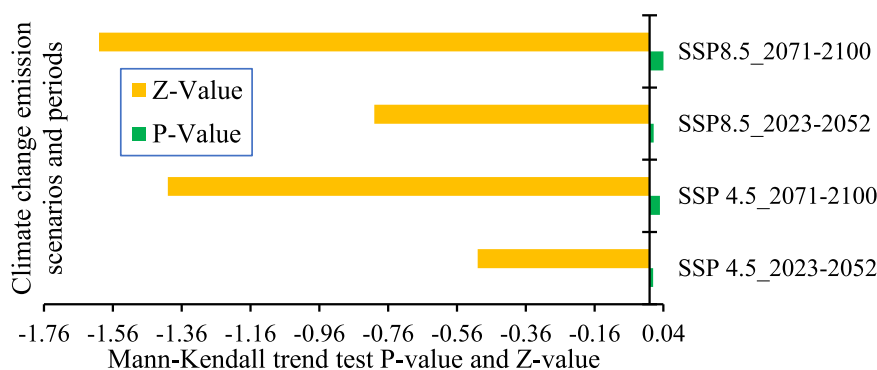


Fig. 15. Projected Seasonal Precipitation Change under SSP_4.5 and SSP_8.5 Emission Scenarios (2023-2052, and 2071-2100).

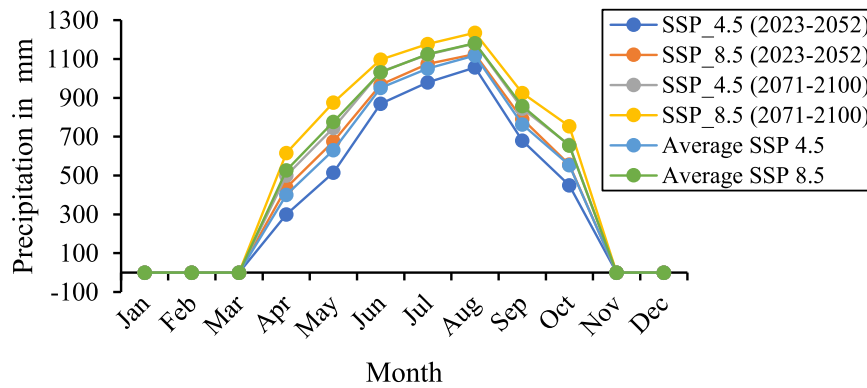


Fig. 16. Projected Changes in Monthly Mean Precipitation under SSP 4.5 and SSP 8.5 Emissions Scenarios (2023-2052 and 2071-2100).

Table 6
Annual and Seasonal Precipitation Projected and Percentage Change.

Year	Referenced, projected yearly total precipitation in (mm)	Projected average change of annual precipitation in (mm)	Projected change in average precipitation in (mm)	Projected change in average precipitation in (%)
Pr_Baseline Period (1993-2022)	11652	-	-	-
Pr_SSP_4.5_2023-2022	10832	902.67	541.6	10.1
Pr_SSP_4.5_2071-2100	9689	807.4	484.44	11.02
Pr_SSP_8.5_2023-2022	10812	901	540.6	13.05
Pr_SSP_8.5_2071-2100	9732	811	486.6	12.03

baseline period, the annual amount and seasonal distribution of the rainy seasons summer from June to August and spring from April to May will decrease in the future.

5.6. Evaluation of observed annual and seasonal stream flow and trend analysis

The variation in annual and seasonal stream flow baselines (2013-2018) over 6 years was statistically analyzed, and statistically significant decreasing trends were found. Fig. 17 displays the data analysis findings, which show a statistically significant downward trend and the reference period for annual stream flow change. Additionally, the trend test analysis revealed that annual and seasonal stream flow will decline over time (Table 7), which is consistent with the two emissions scenarios (SSP 4.5 and SSP 8.5).

5.7. Evaluation of projected annual and seasonal streamflow and trend analysis

Projected annual and seasonal streamflow variations reveal trends that are statistically significant over 60 years (2023-2052 and 2071-

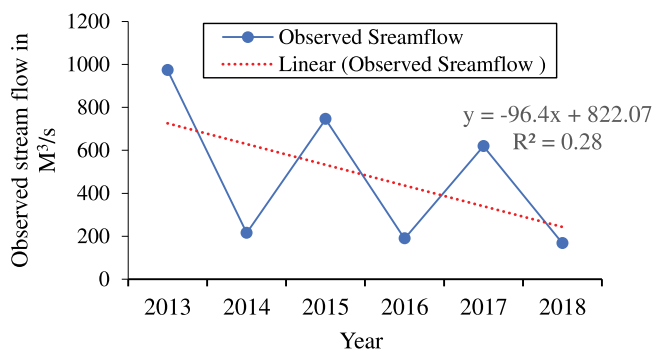


Fig. 17. Historical Annual Stream flow Change in the Baseline Period from (2013–2018).

Table 7
Predicted Changes in Annual and Seasonal Stream flow under SSP 4.5 and SSP 8.5 (2023-2052, and 2071-2100).

Year	Projected annual total streamflow (m³/s)	Monthly average streamflow (m³/s)	Annual Average streamflow change in (%)	Monthly Average Stream flow change in (%)
Reference Period (1993-2022)	900	75	-	-
SSP_4.5_2023-2022	825	64.75	28	5
SSP_4.5_2071-2100	759	63.25	37	5.33
SSP_8.5_2023-2022	813	67.75	36	4.5
SSP_8.5_2071-2100	752	63.67	42	6.12

2100). In (Fig. 18), future periods of streamflow change for the two (2) periods of annual streamflow change are discussed, along with assessment results that show a statistically significant decreasing trend. Additionally, the trend test analysis and assessments show that seasonal streamflow has decreased over the study period under the two (2) SSP 4.5 and SSP 8.5 emissions scenarios (Fig. 19).

The outcomes of this study show decreasing trends over the near future, and far future (2023-2052, and 2071-2100) in (Figs. 18, 19, and 20), which represent the estimated and projected change in average annual streamflow over two-time scales. Overall, the project’s findings showed that under the two (2) SSP 4.5 and SSP 8.5 emission scenarios, annual and seasonal streamflow should be lower than during the historical period (Fig. 20).

For two (2) future periods, as shown in (Table 7), the estimated and projected magnitudes of the seasonal and annual changes in stream flow were evaluated using a variety of techniques. The mean monthly

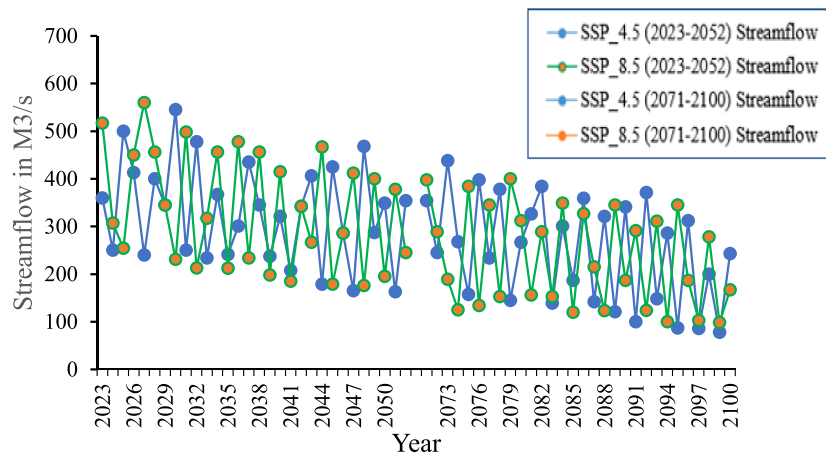


Fig. 18. Projected Changes in Annual Streamflow under SSP 4.5 and SSP 8.5 Emissions Scenarios (2023-2052, and 2071-2100).

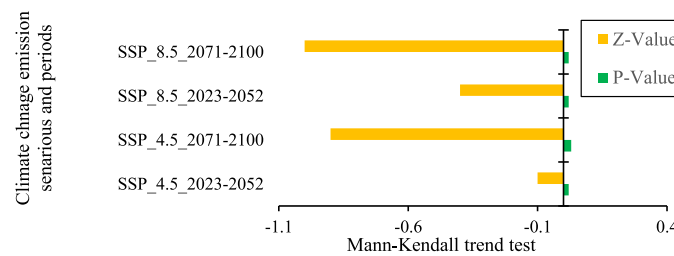


Fig. 19. Change in Predicted Seasonal Streamflow under SSP 4.5 and SSP 8.5 Emission Scenarios (2023-2052, and 2071-2100).

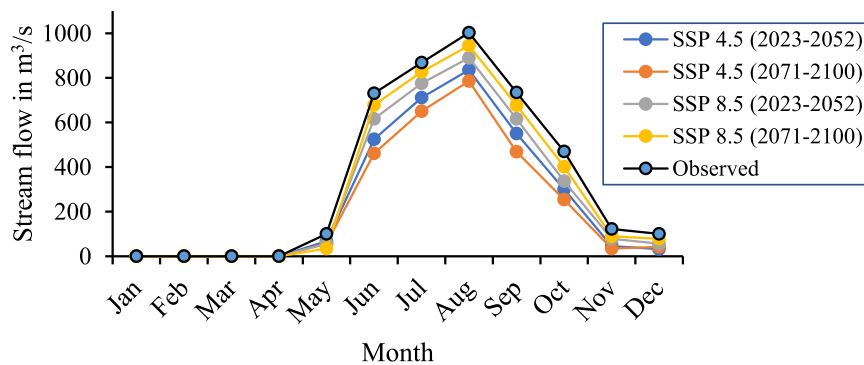


Fig. 20. Projected Changes in Monthly Streamflow under SSP 4.5 and SSP 8.5 Emissions Scenarios during (2023-2052, and 2071-2100).

streamflow during the mean monthly streamflow during the rainy season, and the annual total streamflow were all compared to the baseline period along with the projected streamflow magnitudes and percentage changes. According to projections made under the SSP 4.5 and SSP 8.5 emission scenarios, as shown in (Table 7), the annual and seasonal streamflow magnitude will decrease relative to the reference era for two of the future study periods.

6. Discussions

6.1. The potential climate change impacts on annual and seasonal temperatures

The projected changes in the Veia catchment minimum and maximum temperatures were assessed on an annual, seasonal, and monthly basis. Climate change scenarios SSP 4.5 and SSP 8.5's projected

minimum and maximum temperature changes were evaluated in relation to the baseline. According to projections, annual maximum and minimum temperatures will increase by 34°C, and 28.45 °C under SSP 4.5, while SSP 8.5 will cause an increase of 36 °C, and 29.5 °C throughout future periods, as shown in (Figs. 6 and 7) for the future near future (2023-2052), and far future (2071-2100). The average monthly temperature is predicted to increase by 34°C and 26.45°C under SSP 4.5 and 34°C and 27.5°C according to SSP 8.5, in the years 2023-2052 and 2071-2100 respectively (Figs. 12 and 13). The results are expected to show that over the study periods, the average temperature will increase from 2.10 to 3.5°C in the SSP 4.5 emission scenarios and from 2.4 to 4.15° C in SSP 8.5 emission scenarios. From September to May, the average maximum temperature tends to increase and decrease gradually from June to August. In contrast, the average minimum temperature tends to increase from June to October and decrease gradually from November to December. Compared with the reference period, the

temperature projected from January to May is higher (Fig. 7), and the hot and dry seasons have higher temperatures.

The Veia catchment experiences change in temperature, with a range of 1.6 to 2.8 °C under SSP4.5, and a range of 2.1 to 3.4 °C under SSP8.5. According to studies by Sun et al. (2023), the change in temperature between 2.04 and 4.15 °C by the end of the 2100th century would be nearly identical in direction and time in the SSP 4.5 emission scenarios. The results of other studies have been confirmed by the results of this study. According to Çaktu (2022), the future temperature rise is predicted to be between 2.8 and 5 °C. Ahmed et al. (2015); Amin et al. (2023); Fotso-Nguemo et al. (2023) conducted additional studies focusing on West Africa and predicted future temperature increases. In general, the average temperature changes in the Veia catchment range from 2.1 to 3.5 °C under the SSP 4.5 emission scenarios. However, under the SSP 8.5 emission scenarios, the range is from 2.4 to 4.15 °C by the end of the 2100 century. The findings of this research indicate that the impact of climate change is likely to intensify future water scarcity, as well as lead to increased temperatures and worsening of the hydrological cycle. Due to the impact of increasing temperatures on soil moisture, surface and groundwater, streamflow, and water availability, crops will require a higher amount of water through evapotranspiration.

The anticipated rise in temperature will have an impact on the catchment area's water supply, stream flow, and future amounts of rainfall (Dash & Maity, 2023; Sheikh et al., 2023). The environment experiences several negative effects due to high temperatures. These include reduced moisture in the soil, a rise in the frequency of hot days and a decline in cold days annually, greater evapotranspiration, and limited water accessibility. The amount of water that is accessible will be impacted by changes in precipitation, increasing temperatures, and temperature variations. This is due in part to the expectation that increased temperatures will accelerate the evaporation process. The Veia catchment is expected to face increased water stress and higher temperatures in the coming years.

6.2. Climate change impacts on annual, seasonal and monthly precipitation

On an annual, seasonal, and monthly basis, the projected changes in precipitation for the Veia catchment were assessed for the future near-term (2023-2052), and long-term (2071-2100). During the reference period (1993-2022), the catchment average and annual precipitation were estimated to be 300 mm and 9600 mm, respectively. On the other hand, future forecasts for the near term (2023-2052), and the long term (2071-2100) quantify and project future periods of annual total and average precipitation for the Veia catchment. It was quantified and projected that the annual total and average precipitation would be 10832 and 361 mm, respectively, under the SSP 4.5 emission scenarios and 9689, and 322.96 mm under the SSP 8.5 emission scenarios (Table 6). For the two estimated and projected periods, the amount and distribution of expected climate change effects on future annual precipitation changes are depicted in (Fig. 14) for the SSP4.5 and SSP8.5 emission scenarios. According to all individual and average regional climate model estimates under the SSP 4.5 and SSP 8.5 emission scenarios, precipitation decreased over the next two periods in comparison to the baseline period (Fig. 15). In the near future (2023-2052), and the far future (2071-2100), it is projected that annual precipitation will decrease by 10.01%, and 12.02% under the SSP 4.5 emission scenarios and by 11.05%, and 13.04% under the SSP 8.5 emission scenarios, respectively (Fig. 15).

The results show that the precipitation decreased more significantly under the SSP 8.5 scenario than under SSP 4.5 in the Veia catchment. In comparison to the SSP 8.5 emission scenarios, the projected decreases in mean annual precipitation for the SSP 4.5 emission scenarios range from 12.34 to 13.10%. The mean monthly average precipitation was predicted to decrease by 12.6% and 13.8 %, respectively, for the study periods under the SSP 4.5 and SSP 8.5 emission scenarios (Fig. 15).

According to the SSP 4.5 emission scenarios, the monthly average precipitation changes during the summer's main rainy season will be 10.12 to 11.01 %, while it will be 11.08 to 13.5 % under the SSP 8.5 emission scenarios. Under SSP 8.5 emission scenarios, the window (2071-2100) is expected to have the largest annual precipitation decrease in comparison to the other study windows in the basin (2023-2052). The findings of this study are consistent with previous studies' forecasts of future precipitation declines (Aduku et al., 2023; Agodzo et al., 2023; Capps Herron et al., 2023). Under the SSP4.5 and SSP 8.5 emission scenarios, it is anticipated that future precipitation in the Veia catchment will decrease, during the main rainy season from June to September. The results of this study, which are in agreement with previous studies show that precipitation, or the amount of seasonal precipitation decreases as a result of climate change (Larbi, Obuobie, et al., 2020).

The Veia catchment has only one rainy season from May to mid-October. These rainy seasons are most important because they significantly influence seasonal and annual rainfall patterns during past, present, and projected, and contribute significantly to precipitation and hydrological dynamics. The amount of anticipated precipitation that would result in a future decrease in streamflow will have an impact on the seasonal streamflow's magnitude. As a result, the decrease in precipitation and rise in temperature will have an impact on the catchment's streamflow, available water, irrigation techniques, agricultural output, pasture for the livestock rearing community livelihoods, drinking water, livestock water, and rain-fed agriculture. The results of this study revealed statistically significant relationships between temperature and precipitation. Therefore, future streamflow and water availability in the catchment are directly impacted by the relationship between precipitation and temperature.

6.3. Climate change impacts on annual, seasonal, and monthly streamflow

The projected streamflow for the Veia catchment over the following two time periods near future (2023-2052), and far future (2071-2100) under the SSP 4.5 and SSP 8.5 emission scenarios indicates a decline in the catchment (Fig. 18). Project future streamflow magnitude declines for each scenario over two subsequent periods from the baseline period (Fig. 17). In the future near-term (2023-2052), and far-term (2071-2100) periods, the annual average streamflow is projected to decrease by 163 m³/s and 89 m³/s under the SSP 4.5 emission scenarios, and by 78 m³/s, and 56 m³/s under the SSP 8.5 emission scenarios, respectively, from the baseline period annual average streamflow 167 m³/s. While the projected reduction under SSP 4.5 emission scenarios is 4.5-6.12% over the two (2) study periods, the projected reduction under SSP 8.5 emission scenarios is in the range of 5.0-5.33% for the annual average streamflow decrease. Seasonal streamflow is expected to decline by 2.4-4.2% and 4.5-6.5% under the SSP 4.5 and SSP 8.5 climate change scenarios, respectively. For the study periods, the largest ranges of monthly average streamflow decline under SSP 4.5 and SSP 8.5 are, respectively, 3.45-7.67 % and 6.23-9.8%.

In the near future (2023-2052) and the far future (2071-2100), the highest average monthly discharge, predicted by the SSP 4.5 emission scenarios, will be 64.75 m³/s and 63.25 m³/s. However, the SSP 8.5 emission scenario predicts the highest reduction of 67.75 m³/s and 63.67 m³/s, respectively. The average annual change in streamflow is predicted to decrease from 4.08 to 7.56% under the SSP 4.5 emission scenario and from 6.98 to 8.65% under the SSP 8.5 emission scenario. According to Table 7, in the SSP 4.5 and SSP 8.5 emission scenarios, the predicted mean monthly streamflow change during the rainy season is between 28 and 37% and 36 to 42%, respectively. Expected and projected seasonal streamflow are likely to follow a predicted precipitation pattern, which is expected to vary and decrease across seasons as well as the driest and warmest seasons. The study's findings indicate that the streamflow in the Veia catchment will likely decline in the future. According to (Atulley et al., 2022; Larbi, Obuobie, et al., 2020),

streamflow will change and decline as a result of climate change and its dependence on precipitation. The results of this study support the assertion made in a related study that anticipated decreases in precipitation will be related to future declines in streamflow (Orkodjo et al., 2022; Saeed et al., 2022). This study's conclusions that streamflow changed and decreased under the SSP 4.5 and SSP 8.5 global emissions scenarios are consistent with earlier findings (Swain et al., 2023). This study supported earlier findings that, under both SSP 4.5 and SSP 8.5 climate emissions scenarios, streamflow during rainy seasons would decline significantly in the future (Ji et al., 2022).

According to the research findings mentioned above, the combined effects of rising temperatures and decreasing precipitation will have an impact on streamflow. The results of the study indicate that streamflow is significantly influenced by temperature and precipitation. The finding of (Awotwi et al., 2021), assessment of the effect of climate change on streamflow and this study are in agreement. The study's results also show a significant relationship between streamflow, temperature, and precipitation. Streamflow will decrease when there is less precipitation and more heat. Temperature increases in response to decreased precipitation, illustrating the close relationship between the two elements and restricting future streamflow in the Veja catchment. Future streamflow predictions for the Veja catchment indicate a decline in both annual and seasonal streamflow. This study demonstrated that there is a great deal of uncertainty regarding the streamflow in the Veja catchment in the future. A summary of results evaluated under emission scenarios SSP 4.5 and SSP 8.5, the highly uncertain future streamflow, suggests that climate change may result in water shortages in the catchment.

7. Conclusions

Climate change conditions in the basin were projected using high-resolution GCMs for two emission scenarios SSP 4.5 and SSP 8.5 for two-time windows near future (2023–2052), and far future (2071–2100) compared a project with the reference period (1993–2022). The Mann-Kendall trend test was used to determine whether a change is statistically significant and to detect trends of the baseline line period and future periods of projected temperature, precipitation, and streamflow. Over the two research periods, the estimated and expected annual, seasonal, and monthly temperature changes increased significantly and the expected annual, seasonal, and monthly precipitation and streamflow decreased significantly. The annual and seasonal temperature projections under SSP 4.5 and SSP 8.5 show a statistically significant upward trend. Although the annual and seasonal rainfall and streamflow projections under SSP 4.5 and SSP 8.5 show a statistically significant negative downward trend. Overall, the projected average temperature increase is 1.6–2.8 °C under SSP 4.5 emission scenarios, while 2.1–3.4 °C under SSP 8.5. The projected average annual precipitation decrease range is 10.01–12.02% in the SSP 4.5 emission scenarios whereas the SSP 8.5 emission scenarios decrease range is 11–13.23%. The projected streamflow decrease range is 28–37% under the SSP 4.5 scenario while the SSP 8.5 emission scenario change decrease range is 36–42%. Compared to the reference period, the SSP 8.5 emissions scenarios show significant changes in temperature, precipitation, and streamflow compared to the SSP 4.5 emissions scenarios over two study periods. Streamflow responds linearly to variations in precipitation and temperature. In contrast, the anticipated alterations in precipitation and temperature have a noteworthy impact on the expected change in streamflow.

Streamflow is predicted to decline as temperatures rise and precipitation decreases. Streamflow, precipitation, and temperature had a statistically significant correlation. The findings also revealed a strong relationship between rising temperatures and declining precipitation and streamflow, indicating a major relationship among the two factors that will decrease the catchment's future availability of water. The study's conclusions emphasize the significance of implementing sustainable land and water management in the future to help mitigate the

impacts of climate change. The future will be uncertain as there will be a greater demand for food and water. Changes in the catchment are anticipated, including an increase in temperature rates, a decline in rainfall amounts and distribution, and a decline in streamflow magnitude. We conclude by recommending the earliest possible implementation of feasible and appropriate adaptation and mitigation techniques and actions in order to reduce potential climate change impacts in the Veja catchment.

CRedit authorship contribution statement

Gemechu Fufa Arfasa: Conceptualization, Data curation, Formal analysis, Methodology, Software, Validation, Visualization, Writing – original draft, Writing – review & editing. **Ebenezer Owusu-Sekyere:** Conceptualization, Supervision, Writing – review & editing, Resources. **Dzigbodi Adzo Doko:** Conceptualization, Supervision, Writing – review & editing, Resources.

Declaration of Competing Interest

The authors declare that they have no known competing financial interests or personal relationships that could have appeared to influence the work reported in this paper.

Data availability

The data that has been used is confidential.

References

- Abbaspour, K.C., Rouholahnejad, E., Vaghefi, S., Srinivasan, R., Yang, H., Kløve, B., 2015. A continental-scale hydrology and water quality model for Europe: Calibration and uncertainty of a high-resolution large-scale SWAT model. *Journal of Hydrology* 524, 733–752.
- Adarsh, S., Janga Reddy, M., 2015. Trend analysis of rainfall in four meteorological subdivisions of southern India using nonparametric methods and discrete wavelet transforms. *International Journal of Climatology* 35 (6), 1107–1124.
- Aduku, D., Anaafo, D., Abugre, S., Addaney, M., 2023. Experiential Knowledge of urbanites on climatic changes in the Sunyani municipality, Ghana. *Journal of Urban Affairs* 45 (3), 488–504.
- Agodzo, S.K., Bessah, E., Nyatuame, M., 2023. A review of the water resources of Ghana in a changing climate and anthropogenic stresses. *Frontiers in Water* 4, 973825.
- Ahmed, K.F., Wang, G., Yu, M., Koo, J., You, L., 2015. Potential impact of climate change on cereal crop yield in West Africa. *Climatic Change* 133, 321–334.
- Ali, F., Srisuwan, C., Techato, K., Bennui, A., 2023. Assessment of small hydropower in Songkhla Lake basin. Thailand using GIS-MCDM. *Sustainable Water Resources Management* 9 (1), 25.
- Amin, A., Wane, A., Kone, I., Krah, M., N'Goran, A., 2023. Impacts of climate change on regional cattle trade in the central corridor of Africa. *Regional environmental change* 23 (1), 35.
- Ampadu, B., Boateng, E.F., Abassa, M.A., 2018. Assessing Adaptation Strategies to the Impacts of Climate Change: A Case Study of Pungu–Upper East Region, Ghana. *Environ. Ecol. Res* 6, 33–44.
- Anand, J., Gosain, A.K., Khosa, R., Srinivasan, R., 2018. Regional scale hydrologic modeling for prediction of water balance, analysis of trends in streamflow and variations in streamflow: The case study of the Ganga River basin. *Journal of Hydrology: Regional Studies* 16, 32–53.
- Anteneh, Y., Alamirew, T., Zeleke, G., Kassawmar, T., 2023. Modeling runoff-sediment influx responses to alternative BMP interventions in the Gojeb watershed, Ethiopia, using the SWAT hydrological model. *Environmental Science and Pollution Research* 30 (9), 22816–22834.
- Arnold, J.G., Fohrer, N., 2005. SWAT2000: current capabilities and research opportunities in applied watershed modelling. *Hydrological Processes: An International Journal* 19 (3), 563–572.
- Arnold, J.G., Moriasi, D.N., Gassman, P.W., Abbaspour, K.C., White, M.J., Srinivasan, R., Santhi, C., Harmel, R.D., Van Griensven, A., Van Liew, M.W., 2012. SWAT: Model use, calibration, and validation. *Transactions of the ASABE* 55 (4), 1491–1508.
- Arshad, M., Ma, X., Yin, J., Ullah, W., Liu, M., Ullah, I., 2021. Performance evaluation of ERA-5, JRA-55, MERRA-2, and CFS-2 reanalysis datasets, over diverse climate regions of Pakistan. *Weather and Climate Extremes* 33, 100373.
- Atulley, J.A., Kwaku, A.A., Owusu-Ansah, E.D.J., Ampofo, S., Jacob, A., Nii, O.S., 2022. Modeling the impact of land cover changes on water balance in the Veja catchment of Ghana, 1985–2040. *Sustainable Water Resources Management* 8 (5), 148.
- Awotwi, A., Annor, T., Anornu, G.K., Quaye-Ballard, J.A., Agyekum, J., Ampadu, B., Nti, I.K., Gyampo, M.A., Boakyee, E., 2021. Climate change impact on streamflow in a

- tropical basin of Ghana, West Africa. *Journal of Hydrology: Regional Studies* 34, 100805.
- Beygi, H. (2015). Impact of irrigation development and climate change on the water level of Lake Urmia, Iran. In.
- Boansi, D., Owusu, V., Tham-Agyekum, E.K., Wongnaa, C.A., Frimpong, J.A., Bukari, K. N., 2023. Responding to harvest failure: Understanding farmers coping strategies in the semi-arid Northern Ghana. *Plos one* 18 (4), e0284328.
- Bokhari, S.A.A., Ahmad, B., Ali, J., Ahmad, S., Mushtaq, H., Rasul, G., 2018. Future climate change projections of the Kabul River Basin using a multi-model ensemble of high-resolution statistically downscaled data. *Earth Systems and Environment* 2 (3), 477–497.
- Brouziyne, Y., Abouabdillah, A., Bouabid, R., Benaabidate, L., Oueslati, O., 2017. SWAT manual calibration and parameters sensitivity analysis in a semi-arid watershed in North-western Morocco. *Arabian Journal of Geosciences* 10, 1–13.
- Çaktı, Y., 2022. Identifying impacts of climate change on water resources using CMIP6 simulations. Havran basin case.
- Capps Herron, H., Waylen, P., Owusu, K., 2023. Spatial and temporal variability in the characteristics of extreme daily rainfalls in Ghana. *Natural Hazards* 117 (1), 655–680.
- Carlos Mendoza, J.A., Chavez Alcazar, T.A., Zuñiga Medina, S.A., 2021. Calibration and uncertainty analysis for modelling runoff in the Tambo River Basin, Peru, using Sequential Uncertainty Fitting Ver-2 (SUFI-2) algorithm. *Air, Soil and Water Research* 14, 1178622120988707.
- Chaemiso, S.E., Abebe, A., Pingale, S.M., 2016. Assessment of the impact of climate change on surface hydrological processes using SWAT: a case study of Omo-Gibe river basin, Ethiopia. *Modeling Earth Systems and Environment* 2, 1–15.
- Chen, S., Huang, J., Huang, J.-C., 2023. Improving daily streamflow simulations for data-scarce watersheds using the coupled SWAT-LSTM approach. *Journal of Hydrology*, 129734.
- Dash, S., Maity, R., 2023. Unfolding unique features of precipitation-temperature scaling across India. *Atmospheric Research* 284, 106601.
- Desai, S., Singh, D.K., Islam, A., Sarangi, A., 2021. Multi-site calibration of hydrological model and assessment of water balance in a semi-arid river basin of India. *Quaternary International* 571, 136–149.
- Dessu, S.B., Melesse, A.M., 2013. Impact and uncertainties of climate change on the hydrology of the Mara River basin, Kenya/Tanzania. *Hydrological Processes* 27 (20), 2973–2986.
- Ebrahimian, M., Nuruddin, A.A., Soom, M.A.M., Sood, A.M., Neng, L.J., Galavi, H., 2018. Trend analysis of major hydroclimatic variables in the Langat River basin, Malaysia. *Singapore Journal of Tropical Geography* 39 (2), 192–214.
- Fang, G.H., Yang, J., Chen, Y.N., Zammit, C., 2015. Comparing bias correction methods in downscaling meteorological variables for a hydrologic impact study in an arid area in China. *Hydrology and Earth System Sciences* 19 (6), 2547–2559.
- Farokhnia, A., Morid, S., Abbaspour, K., Delavar, M., 2018. Development of SWAT-LU model for simulation of Lake Urmia water level decrease and assessment of the proposed actions for its restoration; Part 1: Development, calibration and validation of SWAT-LU model. *Iranian Journal of Irrigation & Drainage* 12 (3), 647–665.
- Fotso-Nguemo, T.C., Weber, T., Diedhiou, A., Chouto, S., Vondou, D.A., Rechid, D., Jacob, D., 2023. Projected impact of increased global warming on heat stress and exposed population over Africa. *Earth's Future* 11 (1), e2022EF003268.
- Fukunaga, D.C., Cecilio, R.A., Zanetti, S.S., Oliveira, L.T., Caiado, M.A.C., 2015. Application of the SWAT hydrologic model to a tropical watershed at Brazil. *Catena* 125, 206–213.
- Gassman, P.W., Jeong, J., Boulange, J., Narasimhan, B., Kato, T., Somura, H., Watanabe, H., Eguchi, S., Cui, Y., Sakaguchi, A., 2022. Simulation of rice paddy systems in SWAT: A review of previous applications and proposed SWAT+ rice paddy module. *International Journal of Agricultural and Biological Engineering* 15 (1), 1–24.
- Gaur, S., Bandyopadhyay, A., Singh, R., 2021. Modelling potential impact of climate change and uncertainty on streamflow projections: a case study. *Journal of Water and Climate Change* 12 (2), 384–400.
- Gu, W., Wu, Z., Bo, R., Liu, W., Zhou, G., Chen, W., Wu, Z., 2014. Modeling, planning and optimal energy management of combined cooling, heating and power microgrid: A review. *International Journal of Electrical Power & Energy Systems* 54, 26–37.
- Gumus, V., Avsaroglu, Y., Simsek, O., 2022. Streamflow trends in the Tigris river basin using Mann–Kendall and innovative trend analysis methods. *Journal of Earth System Science* 131 (1), 34.
- Gurara, M.A., Tolche, A.D., Jilo, N.B., Kassa, A.K., 2022. Annual and seasonal rainfall trend analysis using gridded dataset in the Wabe Shebele River Basin, Ethiopia. *Theoretical and Applied Climatology* 150 (1-2), 263–281.
- Gyamfi, C., Tindan, J.Z.-O., Kifanyi, G.E., 2021. Evaluation of CORDEX Africa multi-model precipitation simulations over the Pra River Basin, Ghana. *Journal of Hydrology: Regional Studies* 35. <https://doi.org/10.1016/j.ejrh.2021.100815>.
- Her, Y., Yoo, S.-H., Cho, J., Hwang, S., Jeong, J., Seong, C., 2019. Uncertainty in hydrological analysis of climate change: multi-parameter vs. multi-GCM ensemble predictions. *Scientific reports* 9 (1), 4974.
- Hewitt, C.D., Guglielmo, F., Joussame, S., Bessembinder, J., Christel, I., Doblaz-Reyes, F.J., Djurdjevic, V., Garrett, N., Kjellström, E., Krzic, A., 2021. Recommendations for future research priorities for climate modeling and climate services. *Bulletin of the American Meteorological Society* 102 (3), E578–E588.
- Hosseinzadehtalaei, P., Ishadi, N.K., Tabari, H., Willems, P., 2021. Climate change impact assessment on pluvial flooding using a distribution-based bias correction of regional climate model simulations. *Journal of Hydrology* 598, 126239.
- Ji, H., Peng, D., Gu, Y., Luo, X., Pang, B., Zhu, Z., 2022. Snowmelt Runoff in the Yarlung Zangbo River Basin and Runoff Change in the Future. *Remote Sensing* 15 (1), 55.
- Kikstra, J.S., Nicholls, Z.R.J., Smith, C.J., Lewis, J., Lamboll, R.D., Byers, E., Sandstad, M., Meinshausen, M., Gidden, M.J., Rogelj, J., 2022. The IPCC Sixth Assessment Report WGIII climate assessment of mitigation pathways: from emissions to global temperatures. *Geoscientific Model Development* 15 (24), 9075–9109.
- Kwawuvi, D., Mama, D., Agodzo, S.K., Bessah, E., Issoufou, Y.G., Wisdom, A.S., 2023. Potential catastrophic consequences for rising temperature trends in the Oti River Basin, West Africa. *Frontiers in Climate* 5, 1184050.
- Larbi, I., Forkuor, G., Hountondji, F.C.C., Agyare, W.A., Mama, D., 2019. Predictive Land Use Change under Business-As-Usual and Afforestation Scenarios in the Veia Catchment, West Africa. *International Journal of Advanced Remote Sensing and GIS* 8 (1), 3011–3029. <https://doi.org/10.23953/cloud.ijarsg.416>.
- Larbi, I., Hountondji, F.C.C., Dotse, S.-Q., Mama, D., Nyamekye, C., Adeyeri, O.E., Djan'na Koubodana, H., Odoom, P.R.E., Asare, Y.M., 2021. Local climate change projections and impact on the surface hydrology in the Veia catchment, West Africa. *Hydrology Research* 52 (6), 1200–1215.
- Larbi, I., Nyamekye, C., Dotse, S.-Q., Danso, D.K., Annor, T., Bessah, E., Limantol, A.M., Attah-Darkwa, T., Kwawuvi, D., Yomo, M., 2022. Rainfall and temperature projections and the implications on streamflow and evapotranspiration in the near future at the Tano River Basin of Ghana. *Scientific African* 15, e01071.
- Larbi, I., Nyamekye, C., Hountondji, F.C.C., Okafor, G.C., Odoom, P.R.E., 2020. Climate change impact on climate extremes and adaptation strategies in the Veia catchment, Ghana. *African Handbook of Climate Change Adaptation* 1–17.
- Larbi, I., Obuobie, E., Verhoef, A., Julich, S., Feger, K.-H., Bossa, A.Y., Macdonald, D., 2020. Water balance components estimation under scenarios of land cover change in the Veia catchment, West Africa. *Hydrological Sciences Journal* 65 (13), 2196–2209.
- Le, T.H., Nguyen, T.N.Q., Tran, T.X.P., Nguyen, H.Q., Truong, N.C.Q., Le, T.L., Pham, V. H., Pham, T.L., Tran, T.H.Y., Tran, T.T., 2023. Identifying the impact of land use land cover change on streamflow and nitrate load following modeling approach: a case study in the upstream Dong Nai River basin, Vietnam. *Environmental Science and Pollution Research* 1–14.
- Leta, M.K., Demissie, T.A., Tränckner, J., 2021. Hydrological responses of watershed to historical and future land use land cover change dynamics of Nashe watershed, Ethiopia. *Water* 13 (17), 2372.
- Malik, M.A., Dar, A.Q., Jain, M.K., 2022. Modelling streamflow using the SWAT model and multi-site calibration utilizing SUFI-2 of SWAT-CUP model for high altitude catchments, NW Himalaya's. *Modeling Earth Systems and Environment* 1–11.
- Manski, C.F., Sanstad, A.H., DeCanio, S.J., 2021. Addressing partial identification in climate modeling and policy analysis. *Proceedings of the National Academy of Sciences* 118 (15), e2022886118.
- Masson-Delmotte, V., Zhai, P., Pirani, A., Connors, S.L., Péan, C., Berger, S., Caud, N., Chen, Y., Goldfarb, L., Gomis, M.I., 2021. Climate change 2021: the physical science basis. Contribution of working group I to the sixth assessment report of the intergovernmental panel on climate change 2.
- Meinshausen, M., Nicholls, Z.R.J., Lewis, J., Gidden, M.J., Vogel, E., Freund, M., Beyerle, U., Gessner, C., Nauels, A., Bauer, N., 2020. The shared socio-economic pathway (SSP) greenhouse gas concentrations and their extensions to 2500. *Geoscientific Model Development* 13 (8), 3571–3605.
- Milentijević, N., Valjarević, A., Bačević, N., Ristić, D., Kalkan, K., Cimbaljević, M., Dragojlović, J., Savić, S., & Pantelić, M. (2022). Assessment of observed and projected climate changes in Bačka (Serbia) using trend analysis and climate modeling.
- Nasiri, S., Ansari, H., Ziaei, A.N., 2020. Simulation of water balance equation components using SWAT model in Samalqan Watershed (Iran). *Arabian Journal of Geosciences* 13, 1–15.
- Neitsch, S. L. (2005). *SWAT2005 theoretical documentation*. <http://swatmodel.tamu.edu/media/1292/SWAT2005theory.pdf>.
- Neitsch, S.L., Arnold, J.G., Kiniry, J.R., Williams, J.R., 2011. Soil and water assessment tool theoretical documentation version 2009.
- Oguntunde, P.G., Abiodun, B.J., Lischeid, G., 2017. Impacts of climate change on hydro-meteorological drought over the Volta Basin, West Africa. *Global and Planetary Change* 155, 121–132.
- Okafor, C., Jimoh, O. D., & Larbi, I. (2017). Detecting changes in hydro-climatic variables during the last four decades (1975-2014) on downstream kaduna river catchment, nigeria.
- Orkodjo, T.P., Kranjac-Berisavijevic, G., Abagale, F.K., 2022. Impact of climate change on future precipitation amounts, seasonal distribution, and streamflow in the Omo-Gibe basin, Ethiopia. *Heliyon* 8 (6).
- Pascoe, C., Lawrence, B.N., Guilyardi, E., Juckes, M., Taylor, K.E., 2020. Documenting numerical experiments in support of the Coupled Model Intercomparison Project Phase 6 (CMIP6). *Geoscientific Model Development Discussions* 13 (5), 2149–2167.
- Rahman, K.U., Pham, Q.B., Jadoon, K.Z., Shahid, M., Kushwaha, D.P., Duan, Z., Mohammadi, B., Khedher, K.M., Anh, D.T., 2022. Comparison of machine learning and process-based SWAT model in simulating streamflow in the Upper Indus Basin. *Applied water science* 12 (8), 178.
- Riahi, K., Van Vuuren, D.P., Kriegler, E., Edmonds, J., O'Neill, B.C., Fujimori, S., Bauer, N., Calvin, K., Dellink, R., Fricko, O., 2017. The Shared Socioeconomic Pathways and their energy, land use, and greenhouse gas emissions implications: An overview. *Global environmental change* 42, 153–168.
- Saeed, F.H., Al-Khafaji, M.S., Al-Faraj, F.A., 2022. Spatiotemporal hydroclimatic characteristics of arid and semi-arid river basin under climate change: a case study of Iraq. *Arabian Journal of Geosciences* 15 (14), 1260.
- Shadkam, S., Ludwig, F., van Oel, P., Kirmiz, Ç., Kabat, P., 2016. Impacts of climate change and water resources development on the declining inflow into Iran's Urmia Lake. *Journal of Great Lakes Research* 42 (5), 942–952.

- Sheikh, H.A., Bhat, M.S., Alam, A., Ahsan, S., Shah, B., 2023. Modeling runoff responses to 1.5 C and 2 C rise in temperature in snow-fed basin of western Himalayas. *Sustainable Water Resources Management* 9 (4), 1–15.
- Smitha, P.S., Narasimhan, B., Sudheer, K.P., Annamalai, H., 2018. An improved bias correction method of daily rainfall data using a sliding window technique for climate change impact assessment. *Journal of Hydrology* 556, 100–118.
- Sun, Q., Chen, H., Long, R., Zhang, J., Yang, M., Huang, H., Ma, W., Wang, Y., 2023. Can Chinese cities reach their carbon peaks on time? Scenario analysis based on machine learning and LMDI decomposition. *Applied Energy* 347, 121427.
- Sun, W., Li, Q., Huang, B., Cheng, J., Song, Z., Li, H., Dong, W., Zhai, P., Jones, P., 2021. The assessment of global surface temperature change from 1850s: the C-LSAT2.0 ensemble and the CMST-interim datasets. *Advances in Atmospheric Sciences* 38, 875–888.
- Swain, S.S., Kumar, S.B., Mishra, A., Chatterjee, C., 2023. Sensitive or resilient catchment?: A Budyko-based modeling approach for climate change and anthropogenic stress under historical to CMIP6 future scenarios. *Journal of Hydrology* 622, 129651.
- Sylla, M.B., Nikiema, P.M., Gibba, P., Kebe, I., Klutse, N.A.B., 2016. Climate change over West Africa: Recent trends and future projections. *Adaptation to climate change and variability in rural West Africa* 25–40.
- Trasobares, A., Mola-Yudego, B., Aquilué, N., González-Olabarria, J.R., García-Gonzalo, J., García-Valdés, R., De Cáceres, M., 2022. Nationwide climate-sensitive models for stand dynamics and forest scenario simulation. *Forest Ecology and Management* 505, 119909.
- Wang, F., Shao, W., Yu, H., Kan, G., He, X., Zhang, D., Ren, M., Wang, G., 2020. Re-evaluation of the power of the mann-kendall test for detecting monotonic trends in hydrometeorological time series. *Frontiers in Earth Science* 8, 14.
- Wang, M., Zhang, Y., Lu, Y., Gao, L., Wang, L., 2023. Attribution analysis of streamflow changes based on large-scale hydrological modeling with uncertainties. *Water resources management* 37 (2), 713–730.
- Welde, K., Gebremariam, B., 2017. Effect of land use land cover dynamics on hydrological response of watershed: Case study of Tekeze Dam watershed, northern Ethiopia. *International Soil and Water Conservation Research* 5 (1), 1–16.
- Worqlul, A.W., Ayana, E.K., Yen, H., Jeong, J., MacAlister, C., Taylor, R., Gerik, T.J., Steenhuis, T.S., 2018. Evaluating hydrologic responses to soil characteristics using SWAT model in a paired-watersheds in the Upper Blue Nile Basin. *Catena* 163, 332–341.